



Research Article

## Effects of web openings on axial compression in cold-formed steel lipped channel columns

P. Sangeetha<sup>\*,a</sup>

Department of Civil Engineering, Sri Sivasubramaniya Nadar College of Engineering, Chennai-603 110, Tamil Nadu, India

### Article Info

### Abstract

#### Article History:

Received 14 Dec 2024

Accepted 21 Mar 2025

#### Keywords:

Lipped channel columns;  
Web holes;  
Axial compression;  
Stress distribution;  
Local buckling;  
Finite element analysis

Cold-formed steel (CFS) is widely used in commercial construction due to its structural efficiency, achieved through cold-bending processes, and its adaptability to various prefabricated geometries. However, the introduction of web openings, commonly incorporated for practical purposes such as service integration, can significantly influence the structural performance of CFS columns under axial compression. This study investigates the experimental and analytical behavior of CFS lipped channel columns with web holes, focusing on the effects of hole shape (circular and rectangular) and the number of holes (0, 1, 2, and 3) positioned at equal intervals along the column length. All specimens, fabricated from 2 mm thick channel sections, were subjected to axial compression to evaluate their load-deflection and load-strain responses. The results reveal that web holes affect the load-carrying capacity, with circular holes demonstrating superior performance compared to rectangular ones. Local inward buckling of the web and outward buckling of the flanges were prominent near the web hole regions, particularly for rectangular holes. Finite Element Analysis (FEA) models showed excellent agreement with experimental results, with deviations of less than 4%, validating their predictive accuracy. A comparative evaluation of design codes, including AISI, BS 5950, and Eurocode, highlighted that BS 5950 closely aligns with experimental findings, attributed to its detailed consideration of local buckling effects and conservative safety factors. This study provides valuable insights into the structural behavior of CFS columns with web holes, offering guidance for their design and application.

© 2025 MIM Research Group. All rights reserved.

## 1. Introduction

Cold-formed steel (CFS) has gained widespread popularity in the construction industry due to its high strength-to-weight ratio, ease of fabrication, and versatility in structural applications [1]. Unlike hot-rolled steel, CFS members are manufactured by bending thin steel sheets at room temperature, allowing for a broad range of cross-sectional shapes and geometries. These properties make CFS an ideal choice for modern construction practices, particularly in lightweight and prefabricated structures. In practical applications, CFS members are often designed with web holes to accommodate services such as electrical conduits, plumbing pipes, or HVAC systems. However, these modifications can significantly influence the structural performance of the members, particularly when subjected to axial compression. Web holes introduce stress concentrations, reduce cross-sectional area, and alter the buckling behavior of the member, making it essential to understand and quantify their effects on structural performance.

The incorporation of web holes into CFS members allows for the integration of services such as electrical and plumbing systems, enhancing their functional adaptability. However, the presence of

\*Corresponding author: [sangeethap@ssn.edu.in](mailto:sangeethap@ssn.edu.in)

<sup>a</sup>[orcid.org/0000-0002-7630-011X](https://orcid.org/0000-0002-7630-011X)

DOI: <http://dx.doi.org/10.17515/resm2025-577me1214rs>

Res. Eng. Struct. Mat. Vol. x Iss. x (xxxx) xx-xx

perforations significantly impacts their load-carrying capacity and structural behavior under various loading conditions [2-4]. Previous studies have extensively investigated the effects of perforations on the buckling and post-buckling behavior of CFS members. Crisan et al. [5] conducted numerical simulations to complement experimental findings, providing valuable insights into the structural performance of perforated sections. Similarly, Moen and Schafer [6] introduced the Direct Strength Method (DSM) for designing CFS columns with holes, demonstrating its efficacy in predicting failure loads accurately. The influence of different hole shapes and arrangements on the axial capacity of CFS columns has also been explored, highlighting the critical role of geometric parameters in structural stability [7,8].

Experimental investigations by Tekcham Singh and Singh [9] revealed that perforated tubular stub columns exhibit reduced stiffness and load-carrying capacity compared to solid sections, emphasizing the need for design optimizations to mitigate these drawbacks. Pham et al. [10] further analyzed high-strength CFS channel sections with rectangular and slotted openings, reporting a significant impact of hole geometry on shear and compressive performance. The effects of perforations in CFS channel sections, with and without lips, have been investigated, focusing on failure modes, ultimate strength, and elastic stiffness [11]. Additional studies [12,13] have analyzed the behavior of perforated CFS beams, identifying the critical impact of hole geometry and spacing on the structural response. Reviews of the influence of web holes on CFS columns and beams [14–16] emphasize the need for a detailed investigation of perforation effects under axial compression. A majority of prior works have focused on elliptical web openings, highlighting outcomes from both experimental and analytical investigations. However, comprehensive studies comparing variations in hole shape (e.g., circular and rectangular) and the number of holes in CFS columns under axial compression remain limited.

This study addresses this gap by investigating the structural behavior of CFS-lipped channel columns with web holes under axial compression through both experimental and analytical methods. The key parameters considered include the shape (circular and rectangular) and number of web holes (0, 1, 2, and 3) positioned at equal intervals along the column length. The load-deflection and load-strain characteristics of the columns are analyzed to evaluate the influence of these parameters on the overall performance. Finite element modeling is employed to simulate the experimental conditions, and the results are validated against experimental data.

### **1.1 Novelty and Significance**

This study provides a unique contribution by systematically analyzing the effects of web hole geometry and number on the axial performance of CFS lipped channel columns. Unlike previous works that primarily focus on elliptical holes or isolated cases, this research offers a broader understanding of how circular and rectangular holes influence load-carrying capacity, stiffness, and failure modes. The findings contribute to the development of optimized design guidelines for perforated CFS members, ensuring enhanced structural performance and safety in practical applications.

## **2. Materials and Methods**

### **2.1 Specimen Details**

The cold-formed steel-lipped channel section was selected from the IS 811-1987 [17] 120 x 50 x 15 x 2 mm with pre-punched web holes were tested to failure under compressive loading to find ultimate load, axial compression and strain. The ultimate load-carrying capacity is the maximum load that the column can sustain before failure. The columns were fabricated using CR4-grade steel conforming to IS 513:2008. The circular and rectangular holes were made along the web at the middle, 1/3<sup>rd</sup> and 1/4<sup>th</sup> height of the specimen with center-to-center spacing of 267 mm. The details of the specimen are depicted in Figure 1(a & b). The specifications of all the column specimens are listed in Table 1. The overall length of the specimen was 800 mm. The boundary conditions for the experimental setup simulated hinged supports at both ends of the column. The specimens without web holes were also tested for failure and acted as control specimens for comparison.

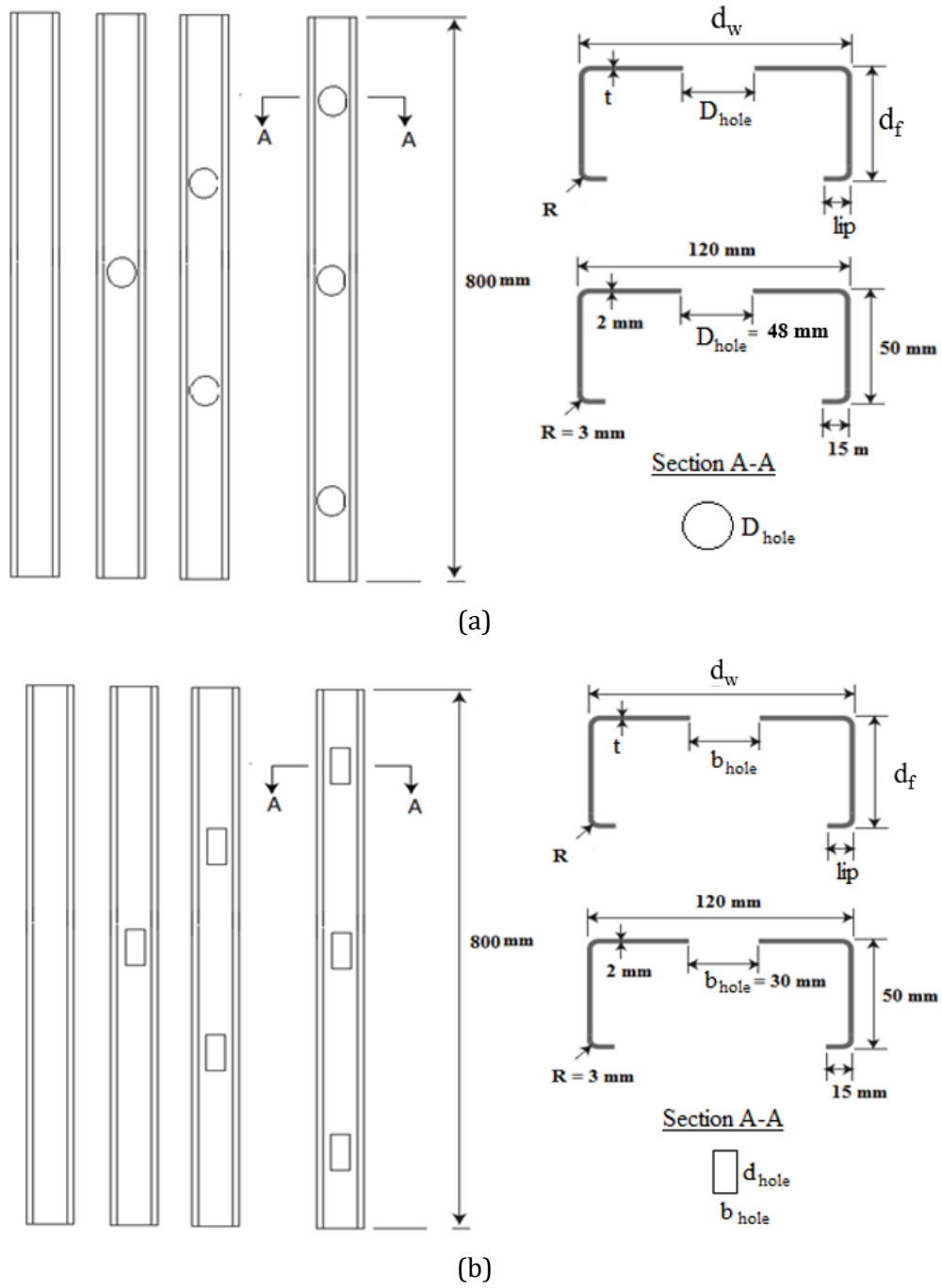


Fig. 1. Specimen dimensions (a) CFST Columns with circular web holes and (b) CFST Columns with rectangular web holes

Table 1. Specification of the specimen

Specimen	L	$b_f$	$d_w$	t	R	Lip	Type of Hole	Number of Hole	$b_{hole}$	$d_{hole}$	$D_{hole}$
									[mm]		
CFSC-0H	800	50	120	2	3	15	-	-	-	-	
CFSC-1RH	801	50	120	2	3	15	Rectangular	1	30	60	-
CFSC-2RH	802	50	120	2	3	15	Rectangular	2	30	60	-
CFSC-3RH	800	50	120	2	3	15	Rectangular	3	30	60	-
CFSC-1CH	799	50	120	2	3	15	Circular	1	-	-	30
CFSC-2CH	801	50	120	2	3	15	Circular	2	-	-	30
CFSC-3CH	802	50	120	2	3	15	Circular	3	-	-	30

## 2.2 Description of the Test

A coupon test was performed for three specimens of standard size as per ASTM E8[18] under a tensile testing machine to know the mechanical properties of the cold-formed steel section. Figure 2 shows the coupon test specimen before and after testing. After testing the stress-strain curve was plotted and it is shown in Figure 3. The yield stress and Young's modulus of materials were found as  $245 \text{ N/mm}^2$  and  $1.95 \times 10^5 \text{ N/mm}^2$  respectively from the stress-strain plot (Fig. 3). All the specimens were fabricated with pre-punched web holes and were shown in Figure. 4. Each specimen was pasted with one 20 mm stain gauge at the mid-height of the specimen to measure the strain along the direction of the application of axial load. The test set-up was employed with a dial gauge with the least count of 0.01 mm to measure the axial compression of the CFS channel section with web holes. Figure. 5 shows that specimen CFSC-2CH was under universal testing machine of capacity 600 kN. and load is applied at the uniform rate of 5kN/mm on the top of the CFS lipped channel section.



Fig. 2. Tensile test on CFS Coupon specimen

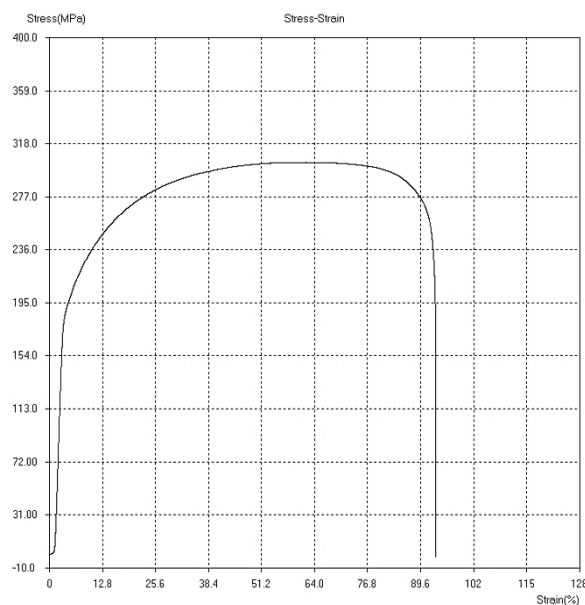


Fig. 3. Stress-strain behaviour of the cold-formed steel



Fig. 4. CFS Column specimens before testing

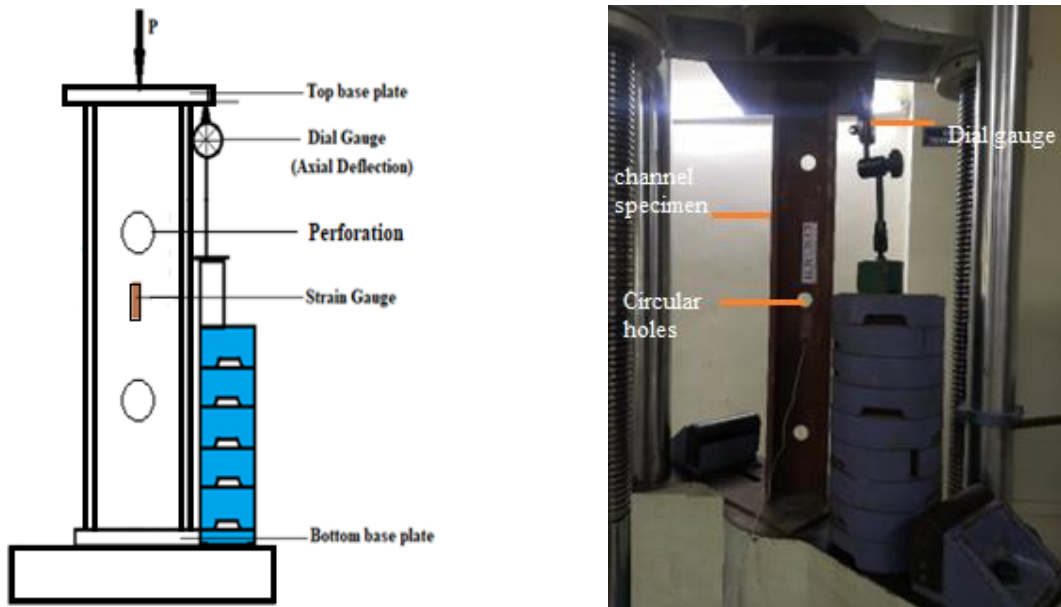


Fig. 5. Experimental set-up

### 3. Numerical Study

Finite Element Analysis (FEA) using ANSYS [19] was conducted to simulate the behavior of cold-formed steel (CFS) lipped channel columns with web holes under axial compression, aiming to replicate experimental conditions and evaluate structural performance. The SHELL 181 element was employed for meshing, offering a balance between computational efficiency and accuracy in capturing membrane and bending effects. A uniform mesh with an element size of 15 mm × 15 mm was applied. Fig. 6 shows the mesh model of the CFS columns with web holes. Material properties were defined using a bilinear stress-strain curve to represent elastic and plastic behavior, incorporating isotropic hardening to account for strain hardening. The elastic modulus was set at 1.95 GPa, Poisson's ratio at 0.3, yield strength at 245 MPa, and ultimate tensile strength at 298 MPa, based on tensile coupon tests for consistency with experimental conditions. Table 2 gives the material properties for FEA.

Table 2. Material properties for FEA

Details	Elastic Modulus	Poisson's Ratio	Yield Strength	Ultimate Tensile Strength	Strain Hardening Modulus	Plastic Strain
	E [GPa]	$\gamma$	$\sigma_y$ [Mpa]	$\sigma_u$ [Mpa]	$E_t$ [Gpa]	$\epsilon_p$
Values	195	0.3	245	298	1.5	0.12

To simulate realistic imperfections, the first buckling mode shape was scaled to a maximum amplitude of  $L/1000$ , where  $L$  is the column length, representing manufacturing defects and initial geometric imperfections. A damage model using a von Mises stress failure criterion was included to predict localized yielding and plastic deformation, capturing the onset of local inward buckling in the web and outward buckling in the flanges. Boundary conditions were applied to replicate the experimental setup, with all translational degrees of freedom ( $U_x$ ,  $U_y$ ,  $U_z$ ) restrained at the top and bottom ends and partial rotational restraint to simulate fixed supports. Axial compression was applied incrementally at the column's top using displacement control to ensure stability during analysis.

The analysis accounted for geometric and material nonlinearities using the Newton-Raphson iterative method, with convergence criteria based on displacement and residual force tolerances set at  $1 \times 10^{-3}$ . The FEA results, including load-deflection and load-strain responses, showed excellent agreement with experimental data, with deviations of less than 4%, validating the model's accuracy. The validated model was then utilized for a parametric study to evaluate the influence of web hole geometry (circular and rectangular) and configurations (0, 1, 2, and 3 holes) on load-carrying capacity, stiffness, and failure modes. This robust methodology bridges experimental and analytical approaches, offering valuable insights into the structural behavior of perforated CFS columns and contributing to the development of efficient design guidelines.

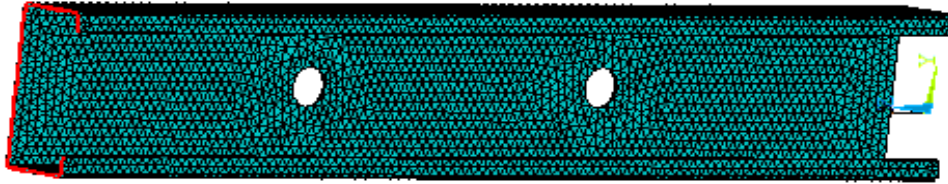


Fig. 6. Finite element mesh model of the CFS column (CFSC-2CH)

## 4. Result and Discussion

### 4.1 Load-Axial Compression Behavior

Figure. 7 (a & b) shows the load-axial compression curve of the CFS columns with circular and rectangular web holes respectively. The stiffness of the CFS column with circular holes is stiffer than the columns with rectangular holes. In the elastic range, axial compression is minimal and increases linearly with load. As the load exceeds the elastic limit, localized buckling or plastic deformation around the holes leads to a non-linear increase in axial compression. Columns with circular holes generally show a more uniform and gradual increase in compression, while rectangular holes cause more abrupt compression due to the higher stress concentrations at the hole corners. The local inward buckling along the web and local outward buckling along the flange at the places of web holes was observed in all the CFS columns both from experimental and analytical studies. This has occurred due to stress concentrations around the holes, which reduce the column's effective stiffness.

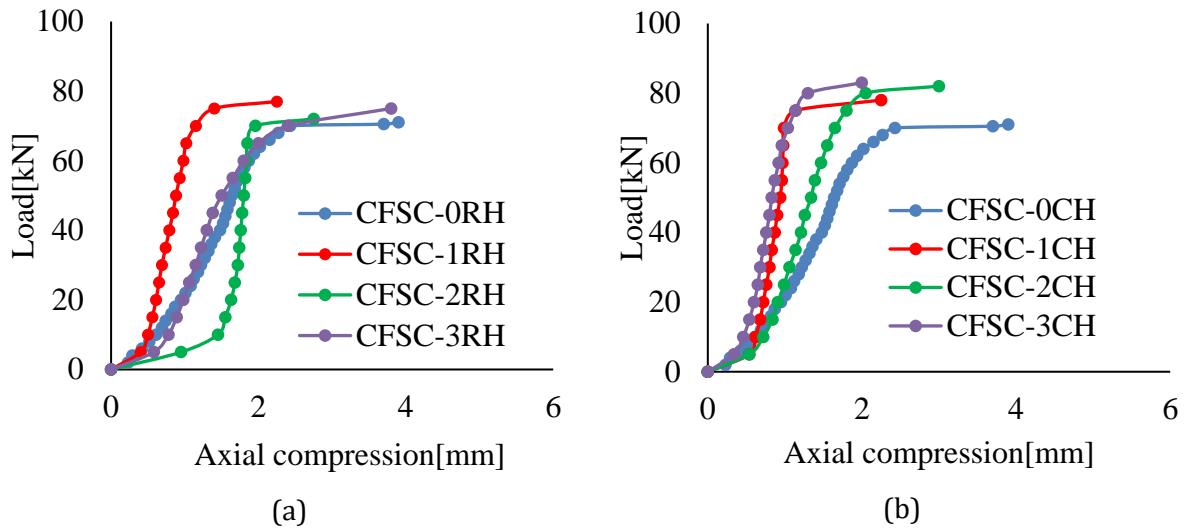


Fig. 7. Load-Axial compression curve of the CFST columns (a) Columns with rectangular web holes and (b) Columns with circular web holes

### 4.2 Load-Micro Strain Behavior

The load versus axial strain curve was plotted for CFS lipped channel columns with rectangular and circular holes using the measured strain from the mid-height of the column with the help of a 20 mm strain gauge. The strain values are recorded in the 5-channel strain indicator. Figure 8(a & b) shows the load versus micro strain plot for CFS columns with rectangular and circular holes. From fig. 8, it was observed that the load-micro strain behavior of cold-formed steel columns reflects the material's response to stress and deformation under increasing load, with notable differences based on the geometry and number of web holes. For circular holes, the strain distribution is more uniform, resulting in a smoother transition from elastic to plastic behavior and delayed strain localization. In contrast, rectangular holes exhibit sharp strain peaks due to stress concentrations at the corners, leading to earlier yielding and non-linear behavior.

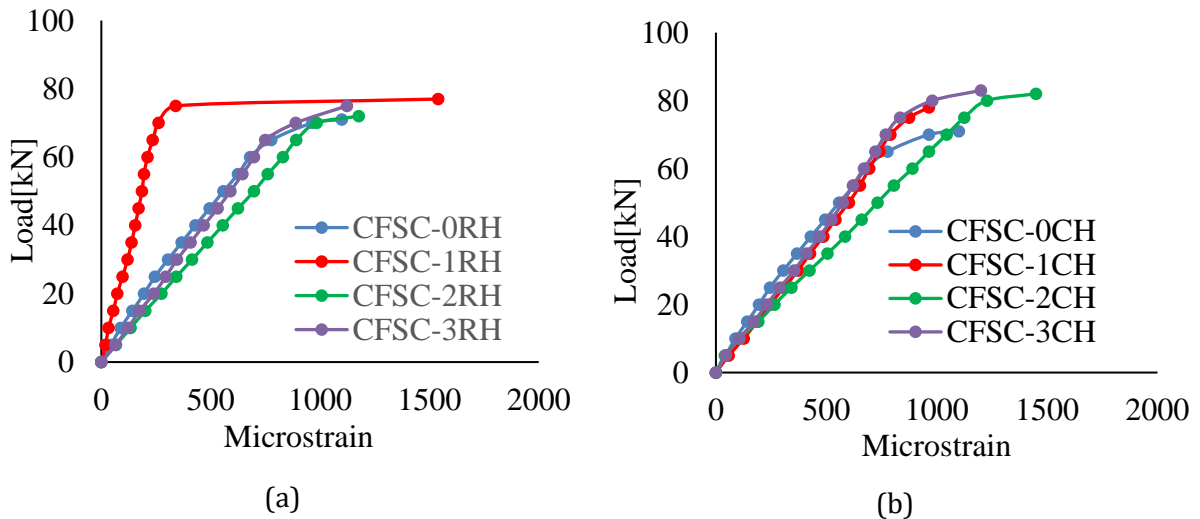


Fig. 8. Load-Micro strain curves of the CFS columns (a) Rectangular web hole and (b) Circular web hole

### 4.3 Effect of Holes in Lipped Channel Column

The load-carrying capacities of cold-formed steel columns with web holes demonstrate a consistent improvement over those without holes. Among the specimens with rectangular holes, CFSC-1RH (1 rectangular hole) showed an 8.45% increase in capacity, while CFSC-2RH (2 rectangular holes) and CFSC-3RH (3 rectangular holes) exhibited increases of 2.82% and 5.63%, respectively. Columns

with circular holes performed even better, with CFSC-1CH (1 circular hole) achieving a 9.86% increase, CFSC-2CH (2 circular holes) achieving 15.49%, and CFSC-3CH (3 circular holes) achieving the highest improvement at 18.31%. These findings indicate that circular holes contribute more significantly to enhancing the load-carrying capacity compared to rectangular holes, and the increase in the number of holes further improves structural performance, with CFSC-3CH emerging as the most efficient configuration. The average percentage increase in the ultimate load-carrying capacity was 10 % for rectangular and circular slotted-lipped channel columns as compared with columns without web holes. The change in the shape of the web holes from rectangular to circular increases the load-carrying capacity by 2%, 14% and 11% for one, two and three holes respectively. This may be due to redistributing stresses and influencing buckling patterns. The presence of multiple circular holes may cause stress redistribution along the web, reducing the concentration of stresses in a single region. This redistribution can lead to better utilization of the material, improving the structural performance under axial loading. Figure 9 shows the variation in the load-carrying capacity between lipped channel sections with and without web holes.

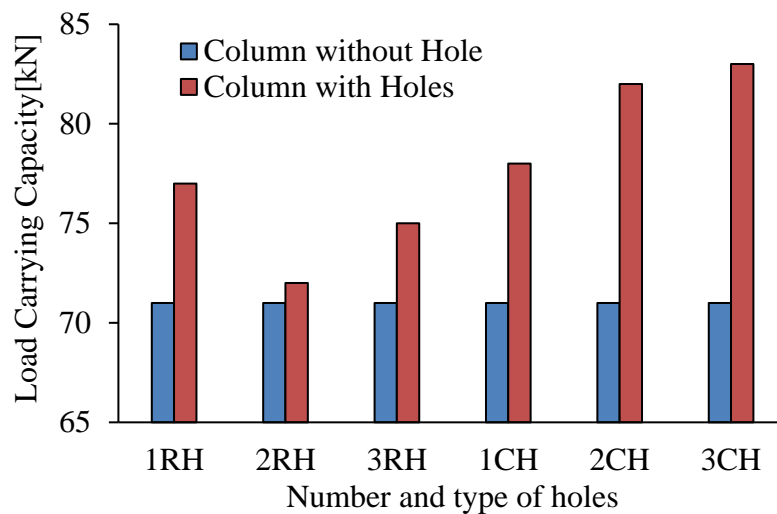


Fig. 9. Comparison between the load-carrying capacity of the slotted CFS columns

#### 4.4 Failure Mode of CFS Column with Web Holes

Figure 10 shows the failure modes of the specimens. The typical failure mode observed was local buckling of the web near the top end of the columns along with inward torsional buckling at the location of web holes. The presence of web holes reduces the web plate transverse stiffness and thus deformation in the web and flange around the hole was more in the columns. These failures were observed on the first web hole from the top of the column as the load was applied at the top. The percentage increase in the load-carrying capacity of CFS columns with circular openings was 12.5 % as compared to rectangular web holes. The reduction in the load-carrying capacity of CFSC-1RH, CFSC-2RH and CFSC-3RH may be due to the weaker axis of the rectangular holes. Thus, the presence of web holes influences the distortional buckling shape and buckling loads.

From the Figure 10, it is also clear that rectangular web holes in the CFS-lipped channel section tend to cause more significant structural performance degradation due to their sharp corners and higher stress concentrations. This leads to earlier yielding and localized buckling, which collectively lower the load-carrying capacity and stability of the column. On the other hand, circular holes distribute stresses more evenly, mitigating some of the adverse effects and generally leading to better performance in terms of structural integrity and resistance to failure.

Figure. 11 shows the deformed plot along the z-axis (axial direction) obtained from the analysis of the CFS columns using ANSYS. From the plot, it was observed that variation in the color shows the intensity of the stress along the axial direction. It was also observed at the location of web holes; the intensity of stress is higher. It shows that dissipation of the stress and energy takes place through the web holes.



Fig. 10. Failure of the perforated CFS columns

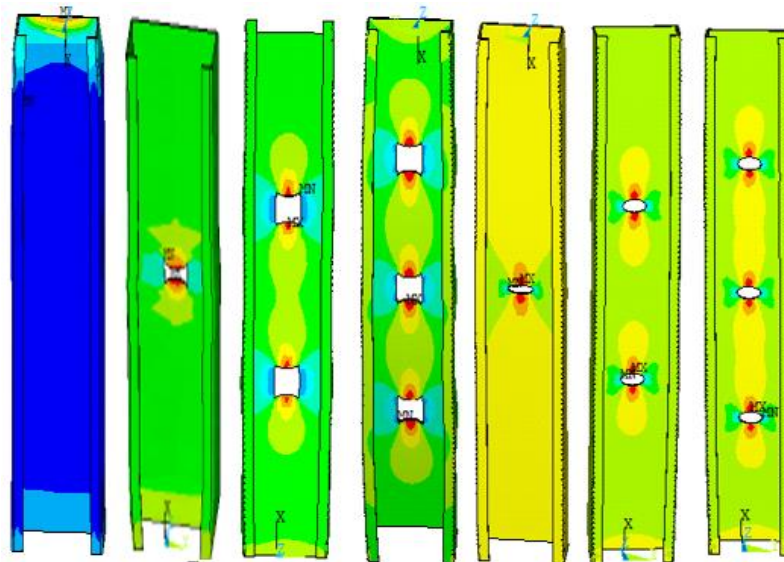


Fig. 11. Stress plot of the CFS columns with and without web holes

Fig. 12 shows the load-axial compression behavior for cold-formed steel columns with web holes (rectangular and circular) between experimental (solid lines) and finite element analysis (FEA) results (dashed lines). The FEA and experimental results show similar trends, validating the FEA model. However, FEA slightly overestimates the ultimate load and underestimates failure displacement, with deviations being more pronounced for rectangular holes due to stress concentrations at sharp corners. Circular holes exhibit better agreement between experimental and FEA results, indicating their superior performance in minimizing stress concentrations. Overall, FEA reliably predicts the behavior of columns with web holes under axial compression.

The ultimate loads of the cold-formed steel channel columns with web holes were calculated using the codal provisions of AISI-2022[20], BS5950[21] and ENV 1993[22]. The correlation between the calculated and experimental values was made and listed in Table 3. From Table 3, it was observed the predicted value using BS 5950 was close to experimental results because the effective width approach in BS 5950 accounts for local buckling effects, which are prominent in cold-formed steel sections. This approach could closely reflect the actual load-carrying behavior of the tested specimens, especially if local buckling dominated failure. The mean and standard deviation were in

the range of 1.016– 1.054 and 0.007 - 0.006 respectively for all the CFS columns with web holes between the predicted and measured values.

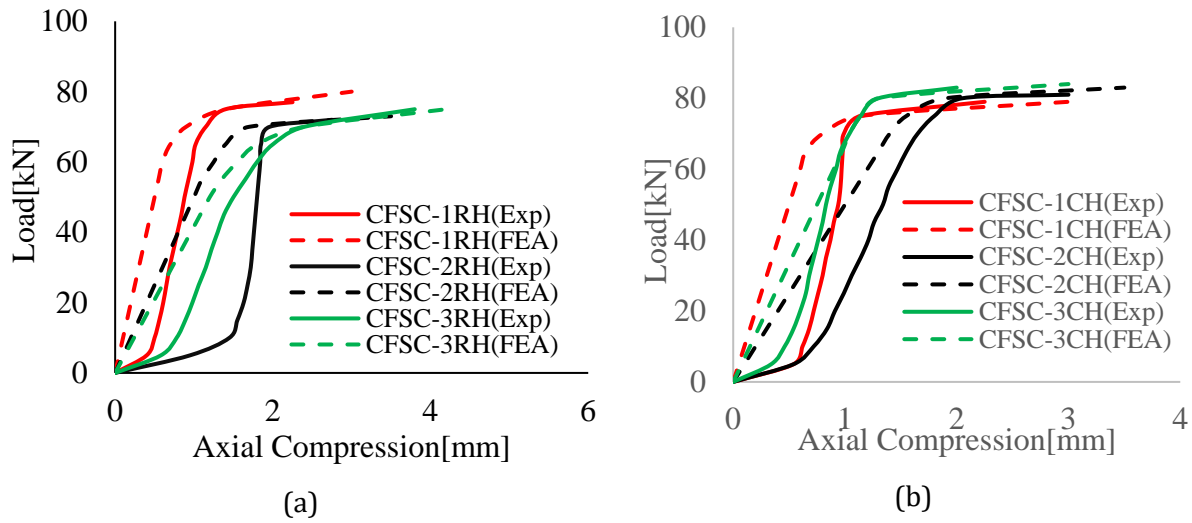


Fig. 12. Comparison between the load- axial compression between Experimental and FEA results

Table 3. Comparison of FEA results and design code calculation with experimental results

Specimen	Maximum load carrying capacity[kN]					Maximum load ratio			
	Test $P_{Exp}$	FEA $P_{FEA}$	AISI $P_{cre}$	BS 5950 $P_c'$	Eurocode $N_{h,Rd}$	$P_{FEA} / P_{Exp}$	$P_{cre} / P_{Exp}$	$P_c' / P_{Exp}$	$N_{h,Rd} / P_{Exp}$
CFSC-0H	71.02	72.51	74.25	71.85	75.24	1.021	1.045	1.012	1.059
CFSC-1RH	77.42	78.35	80.24	77.12	81.25	1.012	1.036	0.996	1.049
CFSC-2RH	72.56	73.01	75.62	73.25	77.26	1.006	1.042	1.010	1.065
CFSC-3RH	75.40	76.21	78.14	75.89	79.25	1.011	1.036	1.006	1.051
CFSC-1CH	78.26	79.56	81.05	79.05	82.25	1.017	1.036	1.010	1.051
CFSC-2CH	82.05	84.01	85.45	82.75	86.02	1.024	1.041	1.009	1.048
CFSC-3CH	83.32	85.21	86.12	82.45	87.52	1.023	1.034	0.990	1.050
	Mean, X					1.016	1.039	1.005	1.054
	Standard Deviation, S					0.007	0.004	0.008	0.006
	Coefficient of Variation, COV					0.007	0.004	0.008	0.006

The study emphasizes that the increase in load-carrying capacity of lipped-channel sections with web openings is a result of the combined effects of stress redistribution, interaction between section components, and optimized material utilization. The experimental and FEA results highlight these effects, which may not be fully captured by simplified design code calculations.

## 5. Conclusions

This study investigated the structural behavior of cold-formed steel (CFS) lipped channel columns with web holes under axial compression using experimental tests and finite element analysis (FEA). The findings reveal the significant influence of hole geometry and number on the load-carrying capacity and failure modes of the columns.

- Columns with web holes exhibited enhanced load-carrying capacities compared to those without holes. Among the tested configurations, CFSC-3CH (3 circular holes) demonstrated the highest increase in load-carrying capacity, achieving an 18.31% improvement over the column without holes.

- Circular holes proved to be more effective than rectangular holes in reducing stress concentrations and improving structural performance. For example, CFSC-2CH showed a 15.49% increase, whereas CFSC-2RH showed only a 2.82% increase in capacity.
- The presence of web holes altered the failure modes of the columns. Local inward buckling of the web and outward buckling of the flanges were more prominent in specimens with rectangular holes, whereas columns with circular holes exhibited more uniform stress distribution and better structural efficiency.
- Finite element analysis results showed excellent agreement with experimental findings, with deviations in ultimate load capacities being less than 4%, validating the accuracy of the FEA model.
- Among the design codes considered, BS 5950 predictions were closest to experimental results, likely due to its consideration of local buckling effects and conservative safety factors.
- The presence of CFS-lipped columns with circular web holes increases the ultimate load-carrying capacity by 10 % when compared to the columns without slotted holes. Rectangular web holes reduced the load-carrying capacity by 10% compared to circular web holes of the same area.
- CFS-lipped channel columns with rectangular holes primarily fail due to localized buckling and crack initiation at the sharp corners, driven by high-stress concentrations. In contrast, columns with circular holes exhibit a more uniform stress distribution, resulting in localized buckling around the hole without crack propagation.
- The load-carrying capacity of all the columns with web holes was also calculated based on the various codal provisions and the coefficient of variation between the calculated and measured experimental values ranged between 0.004 to 0.009.

Future research could explore the behavior of CFS columns with alternative hole shapes (e.g., elliptical or triangular) and varying hole sizes to assess their influence on structural performance. Additionally, parametric studies on different column lengths, end-support conditions, and loading types could provide more comprehensive insights for practical applications. Advanced numerical techniques and optimization algorithms can also be employed to design web hole configurations that maximize structural efficiency while ensuring safety.

## Acknowledgement

The authors would like to thank the management of Sri Sivasubramaniya Nadar College of Engineering for the facilities to complete this research work.

## List of Notations

CFSC	Cold-formed steel column	$d_w$	Web depth of the channel section
RH	Rectangular hole	$t$	thickness of the channel section
CH	Circular Hole	$R$	Corner radius of the channel section
FEA	Finite Element Analysis	$b_{hole}$	breadth of the rectangular web hole
$L$	Length of the column	$d_{hole}$	depth of the rectangular web hole
$b_f$	Flange width of the channel section	$D_{hole}$	Diameter of the circular hole

## References

- [1] Yao X. Experiment and design method on cold-formed thin-walled steel lipped channel columns with slotted web holes under axial compression. *Open Civ Eng J.* 2017;11:244-57. <https://doi.org/10.2174/1874149501711010244>
- [2] Kulatunga MP, Macdonald M, Rhodes J, Harrison DK. Load capacity of cold-formed column members of lipped channel cross-section with perforations subjected to compression loading-part I: FE simulation and test results. *Thin-Walled Struct.* 2014;80:1-12. <https://doi.org/10.1016/j.tws.2014.02.017>
- [3] M.P.Kulatunga & M.Macdonald, Investigation of cold-formed steel structural members with perforations of different arrangements subjected to compression loading, *Thin-Walled Structure*, 67, 2013: pp. 78-87. <https://doi.org/10.1016/j.tws.2013.02.014>

- [4] Kulatunga MP, Macdonald M. Investigation of cold-formed steel structural members with perforations of different arrangements subjected to compression loading. *Thin-Walled Struct.* 2013;67:78-87. <https://doi.org/10.1016/j.tws.2013.02.014>
- [5] Crisan A, Ungureanu V, Dubina D. Behaviour of cold-formed steel perforated sections in compression Part 1-experimental investigations. *Thin-Walled Struct.* 2012;61:86-96. <https://doi.org/10.1016/j.tws.2012.07.016>
- [6] Crisan A, Ungureanu V, Dubina D. Behaviour of cold-formed steel perforated sections in compression Part 2-numerical investigations and design considerations. *Thin-Walled Struct.* 2012;61:97-105. <https://doi.org/10.1016/j.tws.2012.07.013>
- [7] Moen C, Schafer B. Direct strength method for design of cold-formed steel columns with holes. *J Struct Eng.* 2011;137(5):559-70. [https://doi.org/10.1061/\(ASCE\)ST.1943-541X.0000310](https://doi.org/10.1061/(ASCE)ST.1943-541X.0000310)
- [8] Sangeetha P, Dhinakaran M, Gobinaath AS, Saravana Kumar RS, Jeevan Raj AD. Performance assessment of the perforated CFS unlipped and lipped channel section under compression. *Lect Notes Civ Eng.* 2022;179:265-77. [https://doi.org/10.1007/978-981-16-5041-3\\_20](https://doi.org/10.1007/978-981-16-5041-3_20)
- [9] Sangeetha P, Revathi SM, Sudhakar V, Swarnavarshini S, Sweatha S. Behaviour of cold-formed steel hollow beam with perforation under flexural loading. *Mater Today Proc.* 2021;38(5):3103-9. <https://doi.org/10.1016/j.matpr.2020.09.492>
- [10] Singh TG, Singh KD. Experimental investigation on performance of perforated cold-formed steel tubular stub columns. *Thin-Walled Struct.* 2019;131:107-21. <https://doi.org/10.1016/j.tws.2018.06.042>
- [11] Pham DK, Pham CH, Pham SH, Hancock GJ. Experimental investigation of high strength cold-formed channel sections in shear with rectangular and slotted web openings. *J Constr Steel Res.* 2020;165:105889. <https://doi.org/10.1016/j.jcsr.2019.105889>
- [12] Muftah F, Sani MSHM, Kamal MMM. Flexural strength behaviour of bolted built-up cold-formed steel beam with outstand and extended stiffener. *Int J Steel Struct.* 2019;19(3):719-32. <https://doi.org/10.1007/s13296-018-0157-0>
- [13] Ghannam M. Bending moment capacity of cold-formed steel built-up beams. *Int J Steel Struct.* 2019;19(2):660-71. <https://doi.org/10.1007/s13296-018-0155-2>
- [14] Živaljević V, Jovanović Đ, Kovačević D, Džolev I. The influence of web holes on the behaviour of cold-formed steel members: a review. *Buildings.* 2022;12(8):1-33. <https://doi.org/10.3390/buildings12081091>
- [15] Yao Z, Rasmussen KJR. Perforated cold-formed steel members in compression. I: parametric studies. *J Struct Eng.* 2017;134(5):1-15. [https://doi.org/10.1061/\(ASCE\)ST.1943-541X.0001635](https://doi.org/10.1061/(ASCE)ST.1943-541X.0001635)
- [16] Moen CD, Schafer BW. Experiments on cold-formed steel columns with holes. *Thin-Walled Struct.* 2008;46:1164-82. <https://doi.org/10.1016/j.tws.2008.01.021>
- [17] Casafont M, Pastor MM, Roure F, Pekoz T. An experimental investigation of distortional buckling of steel storage rack columns. *Thin-Walled Struct.* 2011;49:933-46. <https://doi.org/10.1016/j.tws.2011.03.016>
- [18] Bureau of Indian Standards. Specification for cold formed light gauge structural steel sections. IS 811-1987. New Delhi; 1987.
- [19] ASTM International. Standard test methods for tension testing of metallic materials. ASTM E8-2016. West Conshohocken, PA; 2016.
- [20] ANSYS. ANSYS Mechanical APDL Structural Analysis Guide: ANSYS Release 21.0. USA; 2021.
- [21] American Iron and Steel Institute. North American cold-formed steel specification for the design of cold-formed steel structural member. AISI-2012; 2012.
- [22] British Standards Institution. British standards for structural use of steel work in buildings - Part 5: Code of practice for design of cold formed thin gauge sections. BS5950-1998; 1998.
- [23] Eurocode 3. Design of steel structures; Part 1.3: General rules - Supplementary rules for cold formed thin gauge members and sheeting. ENV 1993-1-3:2006; 2009.